



Data Article

Experimental investigation of the corrosion inhibition of Aluminum by three novel anionic surfactants as green inhibitors in HCl solution

Mohamed Deef Allah, Manal El Hefnawy^{*}, Samar Abd Elhamed

Basic Science Department, Faculty of Engineering, Shoubra, Egypt

ARTICLE INFO

Keywords:

Anionic surfactants
Eco-friendly
Inhibitors
Aluminum
AFM

ABSTRACT

Based on three different fatty acids and 1, 4 butandiol, three novel anionic surfactants were prepared and examined as an aluminum corrosion inhibitor in 1M hydrochloric acid solution. Weight loss, potentiodynamic polarization, and electrochemical impedance spectroscopy were used to study the corrosion inhibition efficiency (IE %) The results demonstrated that the obtained compounds have good inhibition efficiency even at low concentrations and the IE % increases by increasing inhibitor concentrations, immersion time, and hydrophobic chain length. Also, the obtained compounds behave as mixed-type inhibitors without changing the electrode mechanism. The adsorption mechanism obeys Langmuir adsorption isotherm and the adsorption process is a spontaneous one. Through the biodegradability test, we find that the prepared inhibitors are suitable as environmentally friendly corrosion inhibitors. Finally, atomic force microscopy (AFM) technology was employed to study the impact of the addition of these compounds on the aluminum surface.

1. Introduction

One of the metals that is currently used the most around the world is aluminum, The most prevalent metal in the globe, it makes up around 8% of the planet's crust, and is the third most prevalent element after silicon and oxygen and the world's second-most-used metal after steel because of its favorable traits and adaptability, excellent formability, strong mechanical and electrical conductivity, low weight and high reflectivity [1]. When aluminum is compared to other metals with comparable qualities, it is one of the least expensive, and most abundant [2]. In addition, Aluminum is very resistant to most environments and a wide variety of chemical compounds due to the aluminum oxide layer that grows on the metal's surface which has anti-reactive and preventative properties, but this layer is removed in alkaline and acidic media also in solutions containing chloride.

The use of organic compounds, which create an adsorbing layer that shields the surface of the metal from the corrosive solution is considered the most practical way of preventing aluminum from corroding in an acidic medium [3–16], but most of these substances harm the environment as well as people's health. However, one of the most significant families of organic chemicals utilized as corrosion inhibitors is surfactants because of their lower toxicity, ease of production, and low cost, as well as their greater capacity for adsorbing at the surface of the metal and creating a layer that shields metals from corrosive media [17–25]. Table 1 includes an overview of some articles on the use of polymeric surfactants to prevent aluminum corrosion in HCl.

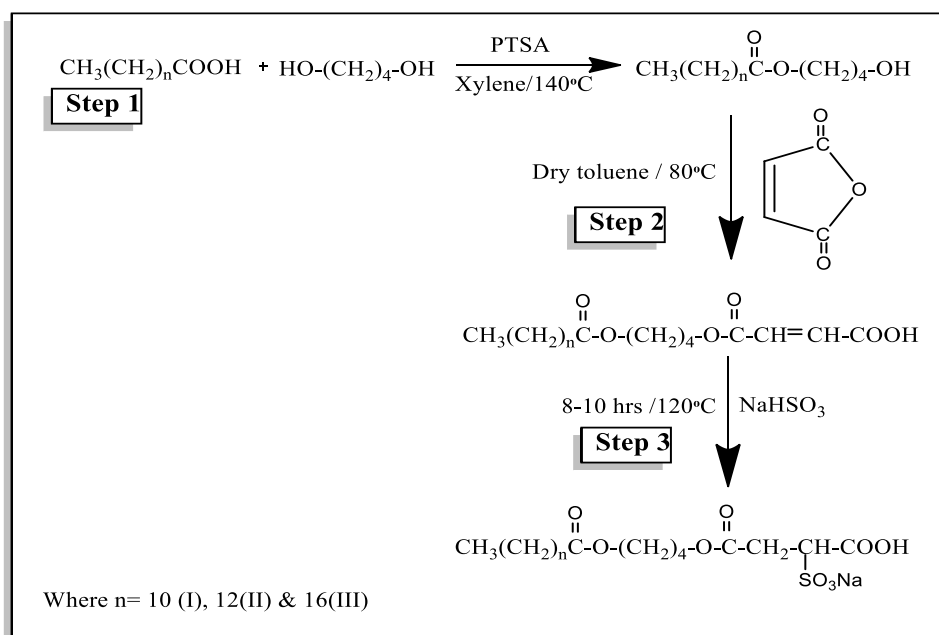
^{*} Corresponding author.

E-mail address: eng.manal.osman@feng.bu.edu.eg (M.E. Hefnawy).

Table 1

some of the previous work on the corrosion inhibition of aluminum using polymeric surfactants.

Materials	Medium	Corrosion inhibitors	Reference
Aluminum	0.5M HCl	3 alkyloxy aniline	[26]
Aluminum	1M HCl	Monomeric surfactant	[27]
		Nonionic surfactant	
		derived from phenol compound	[28]
Aluminum	0.0M HCl	Amido – amine based	
		Cationic surfactant	[29]
Aluminum	1M Hcl	Nonionic surfactant compound with a six membered heterocyclic ring	
Aluminum	1MHCl	Cetyl trimethyl ammonium chloride cationic surfactant	[30]
Aluminum	2MHCl	Bio based nonionic surfactant	[31]
Aluminum	1M HCl	Anionic surfactants from	[32]
		Petroleum oil	
Aluminum	0.5 MHCl	3-(10-Sodium sulfonate decyloxy) Aniline Monomeric Surfactant	[33]

**Scheme 1.** Preparation of the anionic surfactants.

In this study, we developed three environmentally friendly anionic surfactants based on different fatty acids, and we investigated the effectiveness of these compounds to prevent aluminum corrosion in acidic media using a variety of chemical and electrochemical techniques. In addition, the produced surfactants' surface activity, biodegradability and surface morphology were evaluated and linked to their efficacy as inhibitors.

2. Procedure

2.1. Materials

Different fatty acids (lauric, myristic & stearic acid) were obtained from Across Chemical Company (UK). We bought maleic anhydride and 1, 4-butanediol from Sigma-Aldrich (Germany). Fluka Chemika provided Sodium bisulfite and P-toluene sulfonic acid (Germany). The ethanol, xylene, and toluene solvents were dried and provided by (Al-Gomhuria Trade Chemical Company, Cairo, Egypt)

2.2. Synthesis of anionic surfactant

As shown in [Scheme 1](#), there were three major steps in the synthesis of anionic surfactants.

2.2.1. Synthesis of 4-hydroxybutyl dodecanoate, 4-hydroxybutyl tetradecanoate & 4-hydroxybutyl octadecanoate

The intended monoester molecule was produced by allowing 0.1 mol of each of the three separate fatty acids (lauric, myristic, and stearic) to react with 0.1 mol of 1,4 butanediol at 140 °C for 4 h while using 0.1% p-toluene sulphonic acid as a catalysis and 100 mL of xylene as a solvent [34].

2.2.2. Synthesis of the fatty alkyl maleate esters

Maleic anhydride (0.1mol), the synthesized monoesters from step 1(0.1 mol), and dry toluene (50 ml) were all mixed, agitated for 15 min at 80 °C then allowed to stand for 3 h at 25 °C before being kept at 15 °C for an additional 2 h with stirring occasionally. The prepared substance was crystallized by toluene (50 ml) and the product was a white, thick, oily fatty alkyl maleate ester [35].

2.2.3. Synthesis of the final compound

The fatty alkyl maleate esters (0.1 mol) prepared in the previous step (step 2) in 20 ml 95% ethanol were refluxed for 8 hr on a steam bath with Sodium bisulfite (0.1 mol) dissolved in 10 ml water, the reaction filtered hot by suction and treated with 25ml of hot 95% ethanol then cooling in an ice bath and the precipitated materials were filtered and vacuum dried, finally, the product was refined by repeated crystallization from ethyl alcohol [36].

2.2.4. Measurements

The chemical structures of different anionic surfactants were confirmed by FITR and ¹H-NMR spectroscopy. The FTIR measurements were conducted using ATI Mattson Benchtop 961 Infinity Series™ spectrometer equipped with the Win First™ V2.01 Software. Samples were compressed with potassium bromide. The spectra were recorded in the range of 4000 to 400 cm⁻¹.

The ¹H-NMR analysis was performed using a high-performance digital FT-NMR spectrometer (Bruker Avance III 400 MHz) in dimethyl sulfoxide-d₆.

2.3. Corrosion study

2.3.1. Material

The Al electrode used in this study was obtained from the aluminum factory of Nag Hammadi, Egypt with a high purity ratio of 99.99%. For all studies, coupons of 2 cm x 4 cm were mechanically pressed-cut from each Al sheet of 0.1 cm thickness. Aluminum specimens were covered with epoxy resin and subjected to the test solution on a surface area of 1 cm², for the electrochemical examination the coupons were sanded using various emery paper grades (400–1000) before the testing, degreased in 100% ethyl alcohol, dried in acetone, weighed, and then kept dry until use. All solutions used in this study were of analytical grade. Twice distilled water was used for all preparation.

2.3.2. Weight loss measurement

In a weight loss experiment, clean (Al) coupons were weighed and fully submerged in the corroding solution in both the presence and absence of inhibitors. The weight loss (g/cm²) at various immersion periods at 30 °C and IE% were calculated from Eqs. (1) and (2)

$$\Delta W = W_1 - W_2 \quad (1)$$

Where W_1 and W_2 represent, respectively, the specimen's weights before and after being immersed in the corrosive solution [37].

$$\%IE = (\Delta W - \Delta W_i / \Delta W) \times 100 \quad (2)$$

ΔW and ΔW_i are respectively, the weight losses per unit area in the absence and presence of the additive.

2.3.3. Electrochemical measurements

The well-known Origaly French manufacturer potentiostats, galvanostats, and impedance meters (EIS) were used for the electrochemical tests inside a Cap-Services Incubator with a saturated calomel reference electrode (SCE), a platinum counter electrode, and aluminum as the working electrode. Every measurement was performed with 100 cm of 1 M Hydrochloric acid under a constant temperature of 30 °C and 30 min immersion time of the electrode in HCl solution. The electrochemical impedance spectroscopy (EIS) experiment was run using an AC signal amplitude disturbance of 10 mv peak-to-peak within a frequency range of 100 kHz to 0.1 Hz at open-circuit potential (OCP). Data on corrosion were computed using Origa Master 5 software and a Metrohm potentiostat.

2.3.4. Surface properties

A Du-Nouy tension metre was used to measure the surface tension by using the platinum ring detachment method (0.5 mN/m). At 25 °C, fresh aqueous solutions of varying concentrations of the prepared compounds were added to a clean Teflon cup. After being allowed to fully adsorb at the solution surface and stabilize for 2 min, the ring was then cleaned with diluted Hydrochloric acid and distilled water, and the surface tension values were determined using an average of three times [38]. A common surface tension vs. logarithm of surfactant concentration plot was used to determine the CMC values.

2.3.5. Biodegradability

To assess the produced surfactants' capacity to degrade in river water, the Dü-Nouy tensiometer (Krüss type K6) was employed

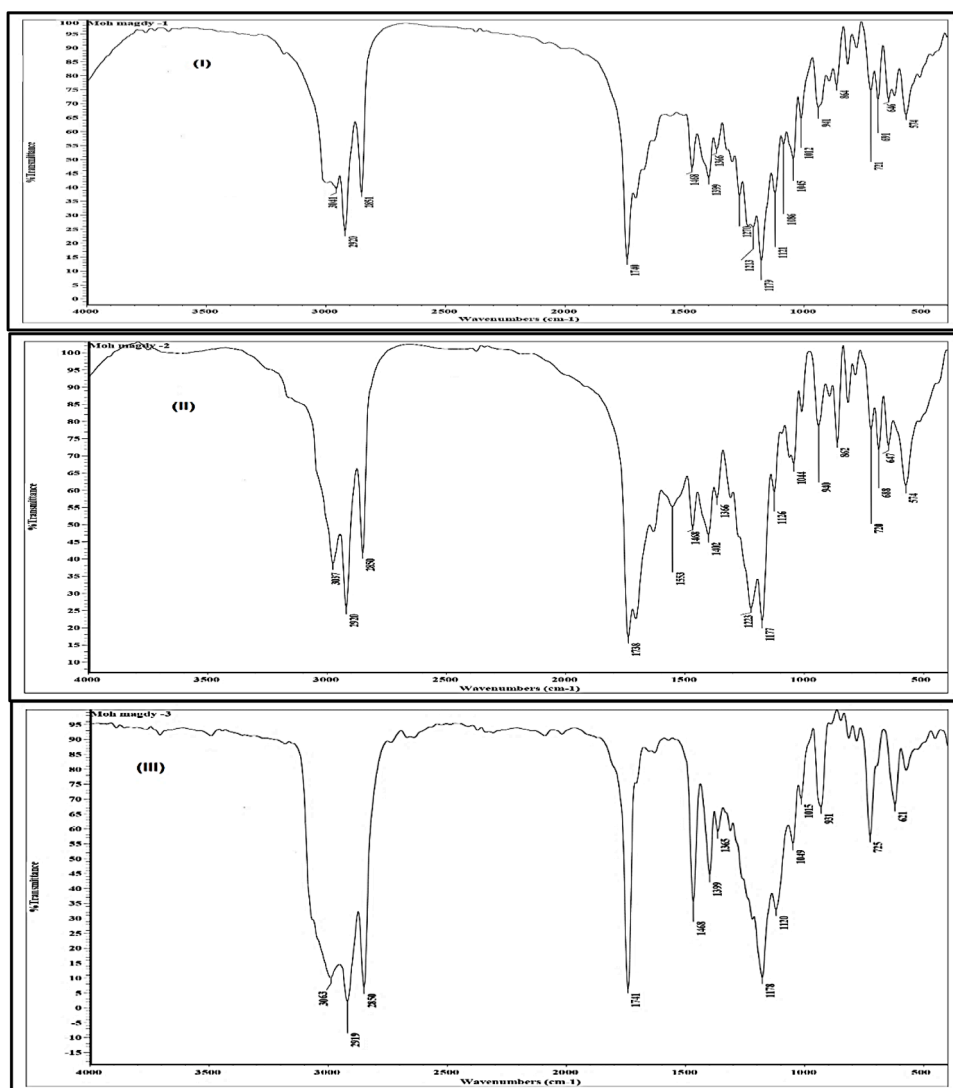


Fig. 1. FTIR spectra of compounds I, II & III.

[39]. For a total of 28 days, a 100 ppm solution of each surfactant was incubated in river water at 30 °C, followed by daily sample withdrawal and filtering to measure the surface tension value. Equation (3) was used to calculate the biodegradation percentage (D %), where γ_o , γ_t and γ_{bt} are the surface tension at zero time, at time t and of the river water respectively

$$D\% = (\gamma_t - \gamma_o) / (\gamma_{bt} - \gamma_o) \times 100. \quad (3)$$

2.3.6. Surface morphology

Atomic force microscopy (AFM; Pico SPM-Pico scan 2100, Molecular Imaging, Arizona, AZ, USA) was used to investigate the surface of aluminum coupons that had been exposed to 1.0 M Hydrochloric acid solutions for 24 h in both the absence and presence of 10^{-3} M of the prepared compound.

3. Results and discussion

3.1. Structure

The chemical structure of the synthesized anionic surfactant was confirmed by FTIR and ^1H NMR

3.1.1. FTIR spectra

FTIR spectrum of the synthesized surfactant (I, II&III) is shown in Fig. 1. Compound I displayed the following absorption bands at

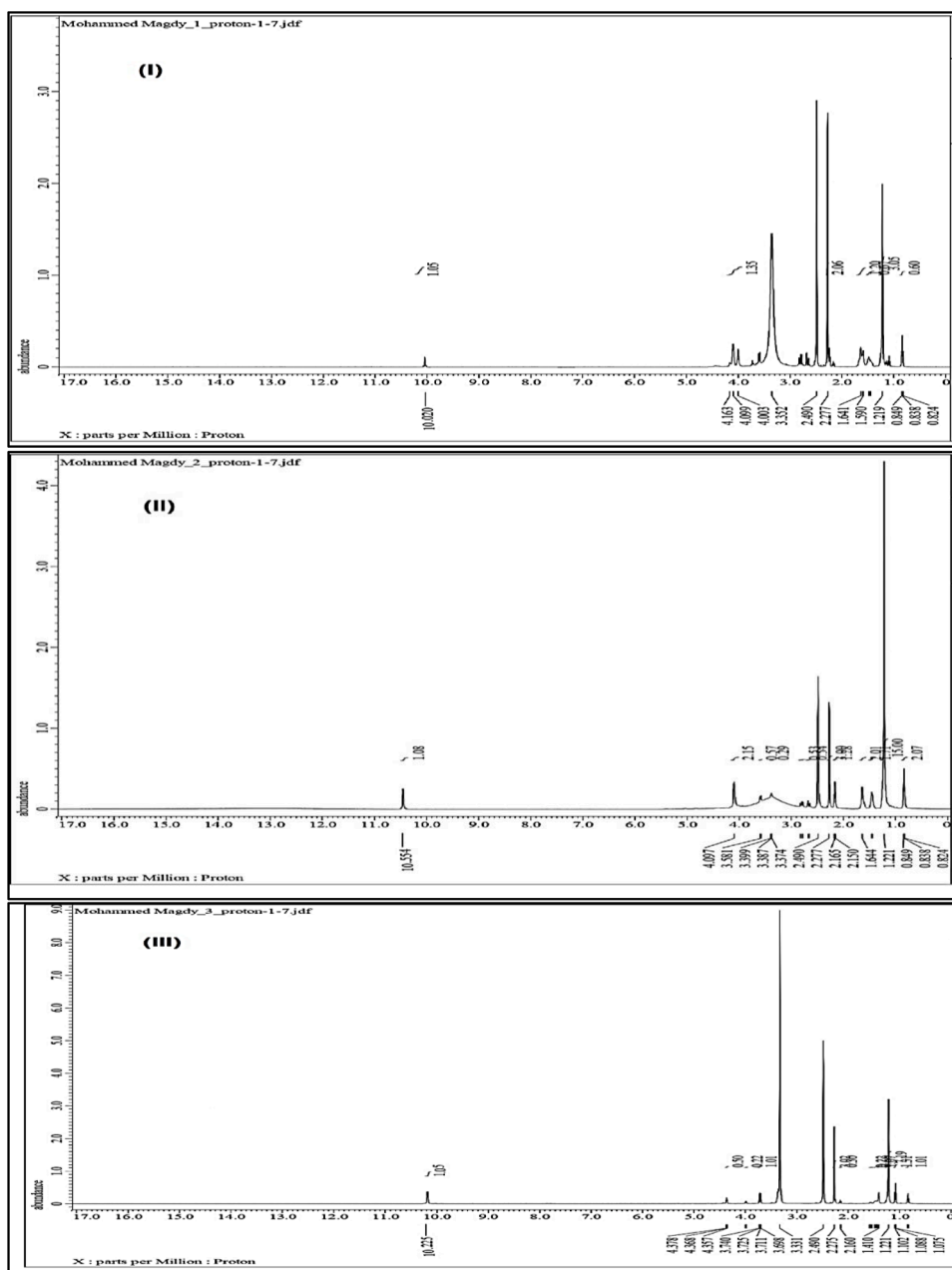


Fig. 2. ^1H NMR spectra of compounds I, II&III.

3041 cm^{-1} was assigned to the hydroxyl group of the acid, 2920 cm^{-1} and 2851 cm^{-1} was ascribed to the CH aliphatic, 1740 cm^{-1} assigned to the carbonyl of the ester group, 1720 cm^{-1} ascribed to the $\text{C}=\text{O}$ of acid, 1468 cm^{-1} C—H bond of CH_2 group, 1179 cm^{-1} (SO_3) sulfonate group, 1121 cm^{-1} and 1086 cm^{-1} were ascribed to C—O—C of ether group and 721 cm^{-1} $[-(\text{CH}_2)_n\text{-skeletal}]$ present in the prepared surfactants.

Compound (II) displayed the following absorption bands: 3037 cm^{-1} , which was assigned to the hydroxyl group of the acid, 2920 cm^{-1} , 2850 cm^{-1} , which was attributed to the CH aliphatic, 1738 cm^{-1} , which was assigned to the carbonyl of the ester group, 1715 cm^{-1} , which were attributed to the $\text{C}=\text{O}$ of the acid, 1468 cm^{-1} , which were assigned to the C—H bond of the CH_2 group, 1177 cm^{-1} (SO_3) sulfonate group, 1126 cm^{-1} and 1044 cm^{-1} were related to C—O—C of ether group and 720 cm^{-1} $[-(\text{CH}_2)_n\text{-skeletal}]$ present in the prepared surfactants.

Compound (III) revealed the successive absorption bands: at 3063 cm^{-1} were assigned to the hydroxyl group of acid, 2919 cm^{-1} and 2850 cm^{-1} were ascribed to CH aliphatic, 1741 cm^{-1} assigned to the carbonyl of the ester group, 1468 cm^{-1} C—H bond of CH_2 group, 1178 cm^{-1} (SO_3) sulfonate group, 1120 cm^{-1} and 1049 cm^{-1} were attributed to C—O—C of ether group and 725 cm^{-1} $[-(\text{CH}_2)_n\text{-skeletal}]$.

Table 2
Effect of the prepared inhibitors concentration on aluminum corrosion.

Inhibitor	Inhibitor concentration (M)	Weight loss (gm/cm ²)	IE %
I	Free	0.8821	-
	10 ⁻⁴	0.4131	53
	5 × 10 ⁻⁴	0.3931	55
	10 ⁻³	0.3110	65
	5 × 10 ⁻³	0.2499	72
	10 ⁻²	0.1552	82
II	10 ⁻²	0.1552	82
	10 ⁻⁴	0.2611	70
	5 × 10 ⁻⁴	0.2510	71
	10 ⁻³	0.2491	72
	5 × 10 ⁻³	0.2335	74
	10 ⁻²	0.1398	84
III	10 ⁻⁴	0.2515	71
	5 × 10 ⁻⁴	0.2467	72
	10 ⁻³	0.2110	76
	5 × 10 ⁻³	0.1631	82
	10 ⁻²	0.1112	87

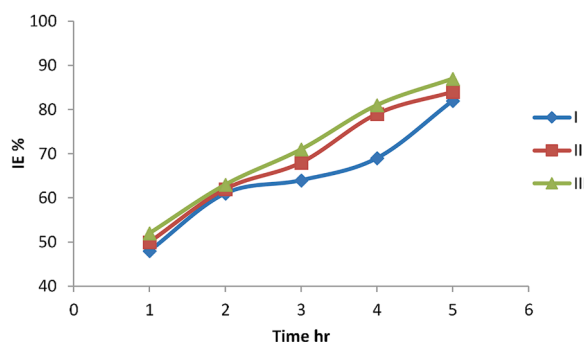


Fig. 3. the relation between inhibition efficiency and immersion time in the presence of 10⁻² M of the prepared compounds.

skeletal present in the prepared compound [40]

3.1.2. ¹HNMR spectra

The synthesized surfactants (I) as in Fig. 2 ¹HNMR (DMSO-d₆) spectrum exhibited various peaks at $\delta = 0.849$ ppm (t, 3H of CH₃); $\delta = 1.219$ ppm (m, 20H) of CH₃—(CH₂)₁₀—; $\delta = 2.49$ ppm (m, 8H of (CH₂)₄); $\delta = 3.352$ ppm (t, 2H of CH₂—CH—COO); $\delta = 4.009$ ppm (t, H of COO—CH₂—CH(SO₃Na)—); and $\delta = 10.02$ ppm (S, 1H of COOH).

The synthesized surfactants (II) as in Fig. 2 ¹HNMR (DMSO-d₆) spectrum exhibited various peaks at $\delta = 0.849$ ppm (t, 3H of CH₃); $\delta = 1.221$ ppm (m, 24H) of CH₃—(CH₂)₁₂—; $\delta = 2.49$ ppm (m, 8H of (CH₂)₄); $\delta = 3.37$ ppm (t, 2H of CH₂—CH—COO); $\delta = 4.097$ ppm (t, H of COO—CH₂—CH(SO₃Na)—); and $\delta = 10.554$ ppm (S, 1H of COOH).

The synthesized surfactants (III) as in Fig. 2 ¹HNMR (DMSO-d₆) spectrum exhibited various peaks at $\delta = 0.85$ ppm (t, 3H of CH₃); $\delta = 1.22$ ppm (m, 32H) of CH₃—(CH₂)₁₆—; $\delta = 2.49$ ppm (m, 8H of (CH₂)₄); $\delta = 3.331$ ppm (t, 2H of CH₂—CH—COO); $\delta = 4.368$ ppm (t, H of COO—CH₂—CH(SO₃Na)—); and $\delta = 10.225$ ppm (S, 1H of COOH) [41]

3.2. Measurements of weight loss

Table 2 lists the data for weight loss and inhibitory effectiveness at various concentrations, it has been noted that as inhibitor concentrations rose, the effectiveness of the inhibition increased as well showing that prepared compounds are acting as good inhibitors. Furthermore, the hydrophobic tail length was correlated with an increase in the inhibitory efficiency with IE percent at 30 °C being III>II>I. As the polar medium and the nonpolar hydrophobic component of the inhibitor repel one another, the aliphatic chain has an impact on corrosion prevention. At the metal/water interface, the hydrophobic chains form a protective layer [42]

The plot of the inhibition efficiencies produced by Eq. (2) against immersion time at constant concentration is shown in Fig. 3. It is clear from the figure That the inhibition efficiency for the three prepared surfactants increases with increasing immersion time; The protective layer that forms on the surface of aluminum is time-dependent, hence the longer the immersion duration, the greater the IE % [43].

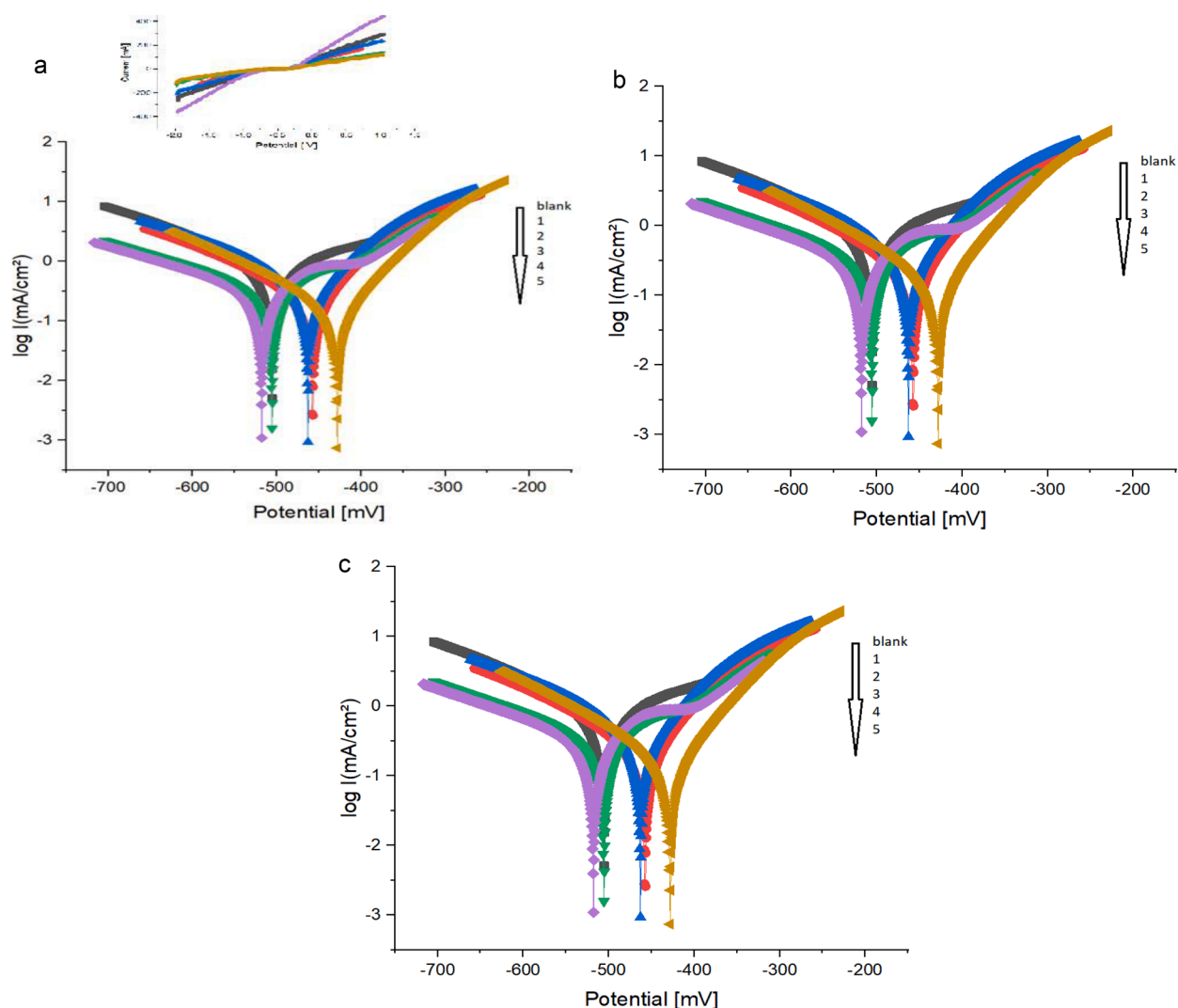


Fig. 4. a. Galvanostatic polarization curves for the corrosion of Al in 1M HCl in the absence and presence of different concentration of compound I (where 1 is 10^{-4} M, 2 is 5×10^{-4} M, 3 is 10^{-3} M, 4 is 5×10^{-3} M, and 5 is 10^{-2} M). b. Galvanostatic polarization curves for the corrosion of Al in 1M HCl in the absence and presence of different concentration of compound II (where 1 is 10^{-4} M, 2 is 5×10^{-4} M, 3 is 10^{-3} M, 4 is 5×10^{-3} M, and 5 is 10^{-2} M). c. Galvanostatic polarization curves for the corrosion of Al in 1M HCl in the absence and presence of different concentration of compound III (where 1 is 10^{-4} M, 2 is 5×10^{-4} M, 3 is 10^{-3} M, 4 is 5×10^{-3} M, and 5 is 10^{-2} M).

3.3. Galvanostatic polarization technique

Figures 4(a, b, c) display the potentiodynamic polarisation curves of Al in 1 M HCl both free and inhibited by the prepared surfactants at different concentrations, it was clear from the figures that the cathodic and anodic polarization curves are both moved to lower current density values also, the dramatic decrease in the cathodic current densities caused by an increase in surfactants concentrations confirms that the inhibition of the cathodic process as a result of adsorption of the prepared compounds on the aluminum surface and the parallel cathodic Tafel curves confirm that the adsorption of these compounds does not effect on the mechanism of the cathodic H_2 evolution [44]. The Tafel curves were used to extrapolate the electrochemical corrosion parameters such as cathodic Tafel slope (bc), anodic Tafel slope (ba), corrosion potential (E_{corr}), and corrosion current density (i_{corr}), also the surface coverage (θ) covered by the synthesized compounds at different concentration individually and the corresponding IE% from polarization measurements were determined using Eqs. (4) and (5) simultaneously, and the results are displayed in Table 3.

$$\theta = (1 - i_{add}/i_{free}) \quad (4)$$

$$\%IE = (1 - i_{add}/i_{free}) \times 100 \quad (5)$$

Table 3

Corrosion parameter obtained from galvanostatic polarization measurements at different concentrations of the prepared inhibitors.

Inhibitor	Conc. (M)	b_a mV dec ⁻¹	$-b_c$ mV dec ⁻¹	$-E_{corr}$ mV (SCE)	I_{corr} (mA cm ⁻²)	%I.E	θ
Blank	—	371.5	225	505.7	1.2	—	—
I	10 ⁻⁴	122.3	212.6	451.1	0.56	53	0.53
	5 × 10 ⁻⁴	155.2	212.4	480.2	0.51	57	0.57
	10 ⁻³	94.2	186.6	433.3	0.41	66	0.66
	5 × 10 ⁻³	98.1	167.6	426.4	0.37	69	0.69
	10 ⁻²	109.8	187.2	455.1	0.27	78	0.78
II	10 ⁻⁴	130.5	237	463.1	0.68	43	0.43
	5 × 10 ⁻⁴	112.7	202.9	457.3	0.36	70	0.70
	10 ⁻³	159.3	242.7	505.6	0.33	73	0.73
	5 × 10 ⁻³	237.4	242.1	517.7	0.31	74	0.74
	10 ⁻²	86.1	168.5	427.7	0.20	83	0.83
III	10 ⁻⁴	118.8	211.2	444.7	0.52	57	0.57
	5 × 10 ⁻⁴	103.9	200.7	447.5	0.41	66	0.66
	10 ⁻³	84.8	171.1	727.2	0.32	73	0.73
	5 × 10 ⁻³	78.9	158.5	430.6	0.21	82	0.82
	10 ⁻²	62.5	131.4	389.6	0.14	88	0.88

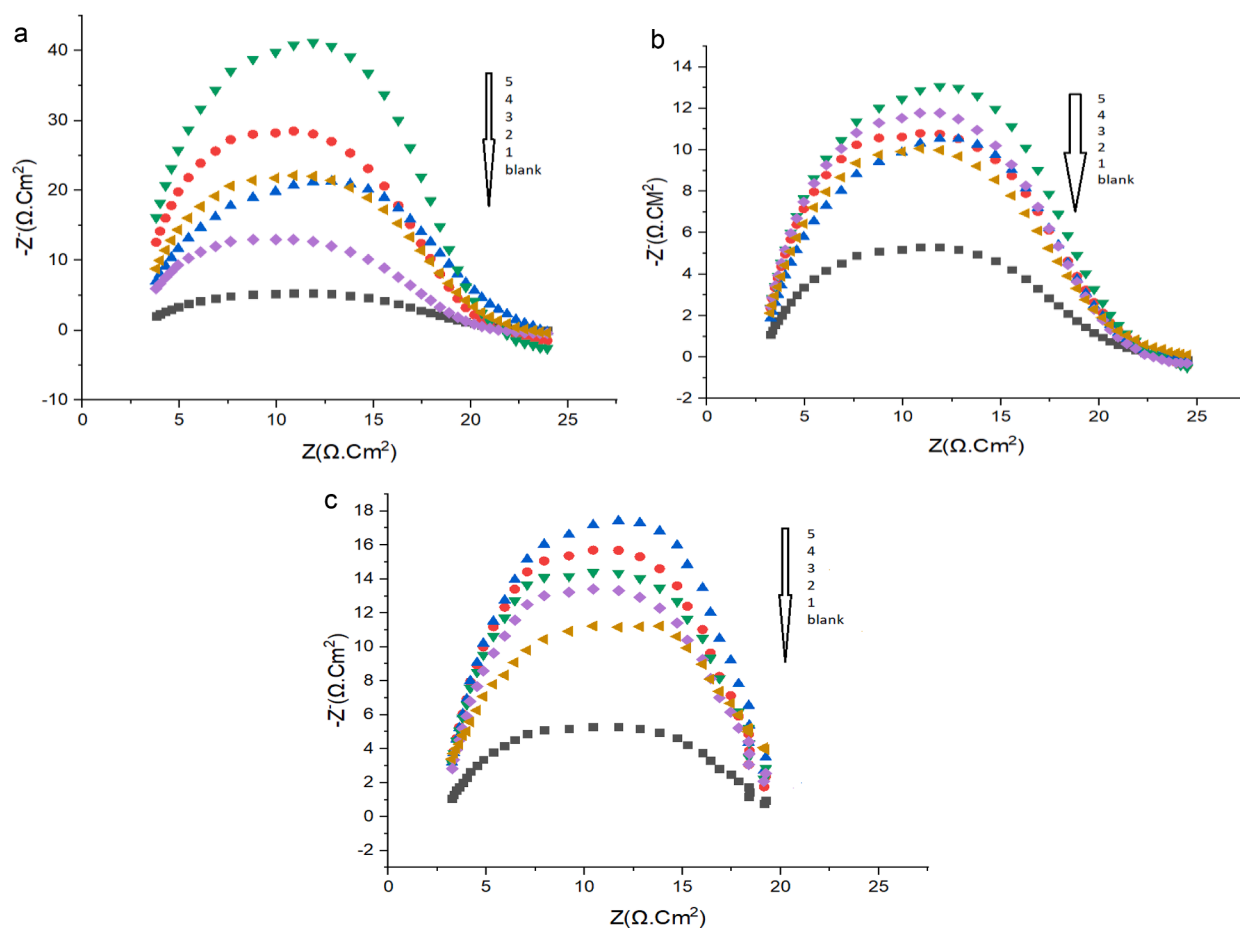


Fig. 5. a. Nyquist curve of Al in 1M HCl in the absence and presence of various amounts of Compound I (where 1 is 10⁻⁴ M, 2 is 5 × 10⁻⁴ M, 3 is 10⁻³ M, 4 is 5 × 10⁻³ M, and 5 is 10⁻² M). b. Nyquist curve of Al in 1M HCl in the absence and presence of various amounts of Compound II (where 1 is 10⁻⁴ M, 2 is 5 × 10⁻⁴ M, 3 is 10⁻³ M, 4 is 5 × 10⁻³ M, and 5 is 10⁻² M). c. Nyquist curve of Al in 1M HCl in the absence and presence of various amounts of Compound III (where 1 is 10⁻⁴ M, 2 is 5 × 10⁻⁴ M, 3 is 10⁻³ M, 4 is 5 × 10⁻³ M, and 5 is 10⁻² M).

Table 4

Electrochemical parameters obtained from EIS measurement for aluminum corrosion in 1.0M HCl at different concentrations of the prepared inhibitors.

Inhibitor	Conc. Of Inhibitor M	$R_{ct}(\Omega \cdot \text{cm}^2)$	$C_{dl}(\mu\text{F}/\text{cm}^2)$	IE%	θ
I	Blank	19.1	398.2	—	—
	10^{-4}	35.2	301.9	45.7	0.457
	5×10^{-4}	40.6	260.6	52.9	0.529
	10^{-3}	44.0	216.3	56.6	0.566
	5×10^{-3}	52.3	188.1	63.5	0.635
II	10^{-2}	81.6	140.5	76.5	0.765
	10^{-4}	38.6	320.5	50.5	0.505
	5×10^{-4}	43.3	273.2	55.9	0.559
	10^{-3}	45.1	237.5	57.6	0.576
	5×10^{-3}	57.4	220.3	66.7	0.667
III	10^{-2}	93.8	170.8	79.8	0.798
	10^{-4}	39.8	339.3	52.0	0.520
	5×10^{-4}	44.4	328.6	56.9	0.569
	10^{-3}	47.8	298.4	60.04	0.600
	5×10^{-3}	59.9	250.3	68.1	0.681
	10^{-2}	102.9	180.3	81.4	0.814

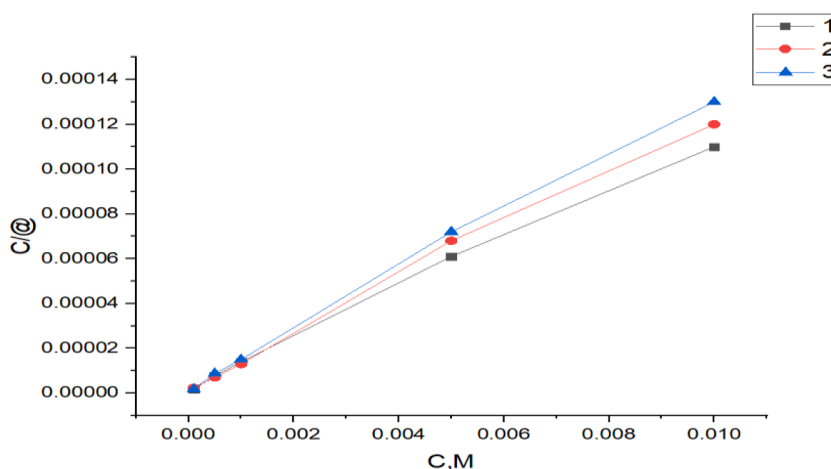


Fig. 6. Langmuir adsorption isotherm (1) Compound I (2) Compound II (3) Compound III.

i_{free} and i_{add} are the corrosion current densities of uninhibited and inhibited metal respectively. It was shown that as the concentration of produced inhibitors increased the inhibitor efficiency (IE%) increased because the inhibitor's capacity to attach to the metal surface was enhanced and a barrier was formed on the surface of Al. Additionally, there was a direct correlation between the IE% and lengthening of the hydrophobic tail of the prepared surfactant. by increasing the hydrophobic tail of the surfactant the IE% increased since as the solution's hydrophobicity rises, more surfactant will migrate to the metal's surface, better shielding the Al surface. At a concentration of 10^{-2} M, the synthesized inhibitors' respective IE% are 78, 83, and 88%. The generated surfactants behave as a mixed-type inhibitors with a predominance of cathodic inhibitor effect because the change in the electrode potentials E_{corr} does not surpass 85 mv when compared to the blank corrosion potential [45–50].

3.4. Electrochemical impedance spectroscopy

The corrosion inhibitory performances of the prepared compounds at various concentrations in 1M HCl at 30 °C are shown in Fig. 5 (a, b, c). It is evident that the Nyquist curves show a depressed capacitive loop, and the radius of the capacitive loop increases as the inhibitor dose increases, indicating that the inhibitors significantly impede charge transfer between the metal and solution. Furthermore, the impedance spectra's shape did not change when the inhibitor was added, indicating that the inhibitor's presence had no bearing on the corrosion mechanism [51–53], the parameters obtained from EIS curve fitting are given in Table 4. And the IE% was determined by Eq. (6) [54,55].

$$\text{IE\%} = \left(\frac{R_{cti} - R_{ctf}}{R_{cti}} \right) \times 100 \quad (6)$$

Where R_{cti} and R_{ctf} are the polarization resistance ($\Omega \text{ cm}^2$) respectively with and without inhibitors. It can be found from Table 4

Table 5
Thermodynamic parameter using Langmuir adsorption isotherm.

surfactants	slope	R ²	Intercept=1/k _{ads}	-ΔG _{ads} ⁰ KJ/mol ⁻¹
I	0.011	0.9974	3*10 ⁻⁶	10.9
II	0.012	0.9960	2*10 ⁻⁶	13.5
III	0.013	0.9974	1.9*10 ⁻⁶	13.9

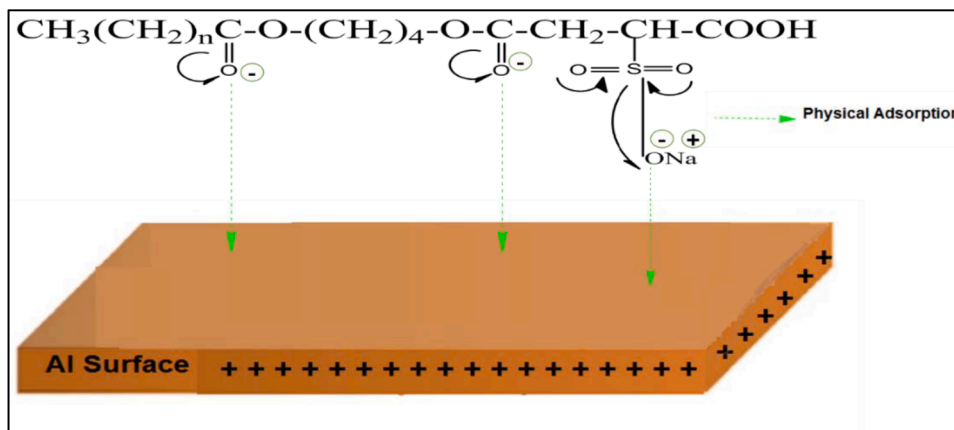


Fig. 7. Schematic diagram representing the adsorption mechanism of the prepared surfactants on aluminum surface.

that with the increase of the inhibitors concentrations the C_{dl} values decrease and the R_{ct} value increases. The increase of R_{ct} is occurred by the gradual displacement of H_2O molecules by the adsorption of the prepared compounds on the Al surface which results in a decrease in the corrosion reaction. Higher values of (R_{ct}) are often linked to a slower corroding process [56]. The fact that the surfactant molecules are operating through absorption at the interface of the Al/solution interface is shown by a decrease in C_{dl} , as a result of the drop in dielectric constant and/or the rise in the thickness of the electrical double layer [57] Finally, the IE% obtained using EIS measurements is comparable to that obtained through polarization measurements and the outcomes of the polarization techniques and weight loss method are consistent with the inhibitory efficiencies estimated from Eq. (6) which followed the order $III > II > I$.

3.5. Adsorption isotherm

An adsorption isotherm can be employed to show the relationship between the inhibitor molecules and the metal surface. A 100% efficiency suggests complete coverage ($\Theta=1$) because the inhibition efficiency is attributed to surface coverage. The Inhibitors' adsorption properties in 1M HCl solution were computed using the degree of surface covering values obtained from Tafel measurements. The pattern of C/Θ against C Fig. 6 displayed a straight line with a correlation coefficient of 0.9999 and a slope almost equal to 1, providing that the adsorption of the prepared surfactants in hydrochloric acid solution on the Al surface obeys Langmuir adsorption isotherm, which is formulated as shown in Eq. (7).

$$C/\theta = 1/K_{ads} + C \quad (7)$$

Where C is the molar concentration of the inhibitors in the bulk solution, θ is the degree of surface covering, and K_{ads} is the equilibrium constant of the adsorption process [58]. To calculate the standard free energy of adsorption ΔG_{ads}^0 , the reciprocal of the intercept values obtained from the plot was employed, ΔG_{ads}^0 , and the adsorption equilibrium constant, K_{ads} , are calculated by Eq. (8).

$$\Delta G_{ads}^0 = -RT \ln(55.5 K_{ads}) \quad (8)$$

as shown in Table 5 the reported negative values of ΔG_{ads} show that the adsorption process is a spontaneous one. According to the previously discussed electrochemical and computational data the inhibitive action of the prepared anionic surfactants in HCl solution results from physical adsorption of the negatively charged sulphonate ions and negatively charged oxygen atom in carbonyl group to the positively charged Al surface as shown in Fig. 7, forming a barrier film on the metal surface which separates the metal from direct corrosion. The values for the standard free energy ΔG_{ads}^0 obtained in Table 5 suggest that the adsorption is of physical type as it is reported in several literature that the values of ΔG_{ads}^0 up to -20KJ/mol are related to the electrostatic interaction (physical adsorption), while further negative values below -40KJ/mol correspond to chemisorption processes [59]. The action of the hydrocarbon chain is to

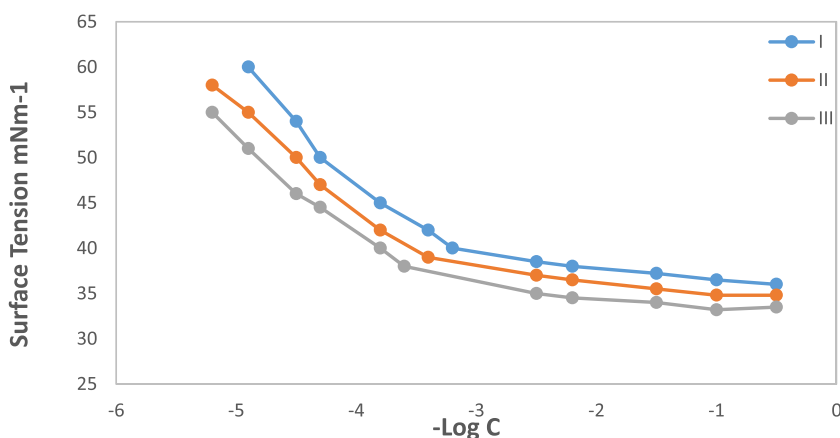


Fig. 8. Dependence of surface tension on the concentration of the prepared surfactants.

Table 6

Surface properties of the prepared inhibitors.

Inhibitor	Surface tension (mN/m) 0.1 wt% at 25 °C	γ_{CMC} (mN/m)	π_{CMC} (mN/m)	CMC (mol/L) $\times 10^{-4}$	$\Gamma_{max} \times 10^{-10}$ (mol/cm ²)	A_{min} (nm ² /mol)
I	36.0	40.1	31.9	6.3	5.17	32.108
II	34.8	39	33	3.98	6.38	26.01
III	33.5	38.2	33.8	2.39	7.207	23.03

Table 7

Biodegradation ratio of the prepared inhibitors at 25 °C.

Inhibitor	7days degradation	14days degradation	21 days degradation	28 days degradation
I	50	61	81	96
II	43	56	74	92
III	39	51	71	87

stabilize the adsorption of the ionic group cohesion on the aluminum surface through Van- der waals force which permits a more densely packed layer at the metal solution interface

3.6. Surface activity

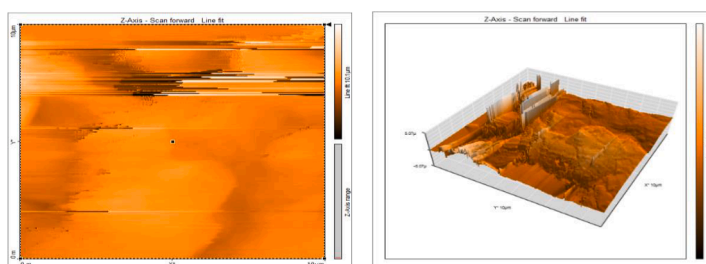
In Table 6, surface tension, CMC, effectiveness (π_{CMC}), maximum surface excess (A_{max}), and minimum area (A_{min}) of the produced surfactants are displayed. It has been demonstrated that the synthesized compounds' surface tensions are less than that of water, indicating that its molecule is capable of being adsorbed at the liquid/air interface. The values for the CMC derived from Fig. 8 are shown in Table 6, the table demonstrates that the surfactant molecule's adsorption at the air-water interface and CMC values reduce as its hydrophobicity rise [60]. The lower CMC values reflect the stronger repulsion between surfactant molecules and water in the aqueous phase which encourages the adsorption of inhibitor molecules on metal surfaces and the formation of the inhibitor monolayers which boosts the effectiveness of inhibitors. Also, according to the estimated π_{CMC} values in Table 6, at the air-water interface, a surfactant with a higher π_{CMC} value will be more likely to be adsorbed than one with a lower π_{CMC} value. It was evident that $III > II > I$ is the sequence in which surfactants can be adsorbed at the interface.

To get A_{min} and Γ_{max} of the surfactant solutions, Gibb's adsorption equations are utilized by Eqs. (9) and (10) [61]

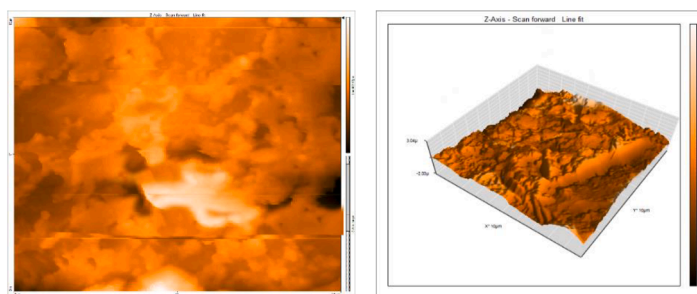
$$\Gamma_{max} = \frac{-1}{RT} \left(\frac{d\gamma}{d\ln C} \right) 100 \quad (9)$$

$$A_{min} = \frac{10^{14}}{\Gamma_{max} \times N} \quad (10)$$

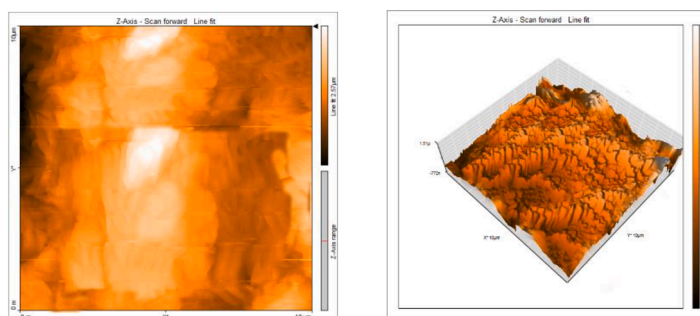
Where C is the concentration of surfactant, R is the gas constant, N is Avogadro's number, T is the absolute temperature, and $d/d\ln C$ is the slope of the plotted γ against $\log C$ in each case It can be seen from Table 6 that The value of Γ_{max} increases while the A_{min} decrease as the surfactants' hydrophobic chain length increase. Increasing solution hydrophobicity enhance the migration of surfactant molecule to the surface therefore a high dense layer is predicted to construct with a higher surfactant tail. The four values of CMC, π_{CMC} , Γ_{max} and A_{min} are arranged in the same order as the sequences of the IE % of the prepared inhibitors, as was discovered



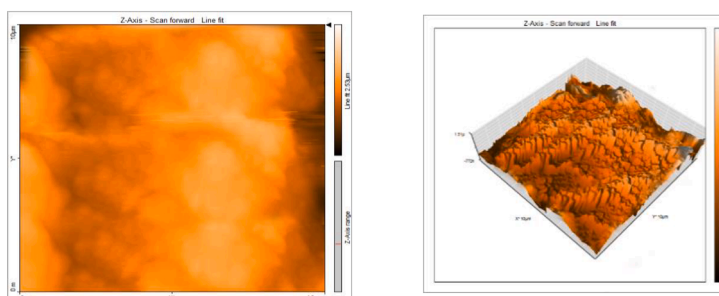
(a) Blank 2D & 3D respectively



(b) compound I 2D & 3D respectively



(c) Compound II 2D & 3D respectively



(d) Compound III 2D and 3D respectively

Fig. 9. 2D and 3D atomic force images for aluminum surface after immersion in 1 M HCl (a) blank (b) inhibited with compound I (c) inhibited with compound II (d) inhibited with compound III.

from the aforementioned data.

3.7. Biodegradation

According to the data in Table 7, all produced compounds had a biodegradation ratio ranging from 87 to 96% following 28

Table 8
AFM roughness data of the prepared inhibitors.

Inhibitor	Area, pm ²	Sa (nm)	Sp (nm)	Sv (nm)
Blank	100.8	589.14	50681	-5068.1
I	100.8	217.25	1112.8	-2172.1
II	100.8	206.63	1060.3	-2269.4
III	100.8	141.22	1014.3	-2427.4

exposure days to microorganisms. Additionally, the maximum biodegradation ratio was reached for compound I, which has a low hydrophobic character. The biodegradation ratios are within the recommended range of 70% after 28 days for biodegradable surfactants in drain water [62]. This makes these surfactants a class of biodegradable surfactants.

3.8. Surface examination

AFM is an essential technique for obtaining knowledge of metal surfaces. Such technology is helpful for corrosion research since it provides a wealth of data on the roughness of the surface being researched [63]. The metal specimens utilized to analyze the surface morphology were employed to make both the three-dimensional and two-dimensional photographs for the Al surface coupons after being immersed in 1 M Hydrochloric acid in the absence and in the presence of 10^{-2} M of the produced compounds at 25 °C for 5 h. Fig. 9 shows how using inhibitors greatly reduces the roughness of the aluminum surface by covering the metal surface and protecting it from the corrosive solutions, the degree of roughness increases from free > I > II > III. The roughness data for aluminum samples are displayed in Table 8. The table displays the peak height (Sp), average roughness (Sa), and valley depth (Sv). The data showed that all measured values were arranged in a certain order, free > I > II > III, beginning with the blank sample and finishing with the inhibited one. It is clear also, that the metal surface becomes smoother after applying the generated compounds because the compound's molecules adhere to the metal surface. Additionally, the efficacy of surfactant rises in a similar way to the efficacy of the inhibition produced by electrochemical and weight loss approaches.

4. Conclusion

- 1 Even at low concentrations, the prepared compounds effectively prevent aluminum from corroding in an acidic solution.
- 2 Corrosion prevention efficiency rises with concentration, immersion duration, and hydrophobic chain length.
- 3 The synthesized compounds are mixed-type inhibitors, according to the results of electrochemical methods, and the inhibition efficiencies identified by weight loss measures and electrochemical methods were compatible with one another and occurred in the following order: III > II > I.
- 4 The adsorption of the synthesized anionic surfactant molecules on the metal surface obeys the Langmuir adsorption isotherm. Inferred from the negative value of ΔG_{ads} is that the adsorption process is spontaneous.
- 5 According to the biodegradability test, these compounds are environmentally friendly
- 6 An AFM analysis of the surface morphology reveals that the application of compounds considerably reduces the roughness of the aluminum surface and that the addition of the prepared compounds results in a smoother surface due to adhering of its molecules to the Al surface.
- 7 The efficiency of surfactants rises in the same order as the inhibitory effectiveness acquired by weight loss and electrochemical methods

Declaration of Competing Interest

We declare that this manuscript is original, has not been published before and is not currently being considered for publication elsewhere. There has been no significant financial support for this work that could have influenced its outcome, and I confirm that the manuscript has been read and approved for submission by all the named authors.

Data availability

No data was used for the research described in the article.

References

- [1] J.D. wight, *Aluminum Design and Construction*, CRC Press, 2002.
- [2] K. Khanari, M. Finsgar, Organic corrosion inhibitors for aluminum and its alloys in chloride and alkaline solutions: a review, Arab. J. Chem. 12 (8) (2019) 4646–4663, <https://doi.org/10.1016/j.arabjc.2016.08.009>.
- [3] M. Abdallah, E.A.M. Gad, J.H. Al-Fahemi, M. Sobhi, Experimental and theoretical investigation by DFT on the some azole antifungal drugs as green corrosion inhibitors for aluminum in 1.0M HCl, Prot. Met. Phys. Chem. Surf. 54 (2018) 503–512, <https://doi.org/10.1134/S207020511803022X>.
- [4] M. Abdallah, Antibacterial drugs as corrosion inhibitors for corrosion of aluminum in hydrochloric solution, Corros. Sci. 46 (2004) 1981–1996, <https://doi.org/10.1016/j.corsci.2003.09.031>.

- [5] X. Deng, S. Li, H. Fu, Inhibition by tetradecylpyridinium bromide of the corrosion of aluminum in hydrochloric acid solution, *Corros. Sci.* 53 (2011) 1529–1536, <https://doi.org/10.1016/j.corsci.2011.01.032>.
- [6] S. Safek, B. Duran, A. Yurt, G. Turkoglu, Schiff bases as corrosion inhibitor for aluminum in HCl solution, *Corros. Sci.* 54 (2012) 251–259, <https://doi.org/10.1016/j.corsci.2011.09.026>.
- [7] N.O. Eddy, H.M. Yahya, E.E. Oguzie, Corrosion Inhibition properties of norepinephrine molecules on mild steel in acidic media, *J. Encapsulation Ads. Sci.* 5 (2015) 155–164, <https://doi.org/10.4236/jeas.2015.53013>.
- [8] M. Abdallah, M. Sobhi, H.M. Altass, Corrosion inhibition of aluminum in hydrochloric acid by pyrazinamide derivatives, *J. Mol. Liq.* 223 (2016) 1143–1153, <https://doi.org/10.1016/j.molliq.2016.09.006>.
- [9] N.M. Likhonova, P. Arellanes-Lozada, Effect of organic anions on ionic liquids as corrosion inhibitors of steel in sulfuric acid solution, *J. Mol. Liq.* 279 (2019) 267–278, <https://doi.org/10.1016/j.molliq.2019.01.126>.
- [10] H. Allal, Y. Belhocine, E. Zouaoui, Computational study of some thiophene derivatives as aluminum corrosion inhibitors, *J. Mol. Liq.* 265 (2018) 668–678, <https://doi.org/10.1016/j.molliq.2018.05.099>.
- [11] D. Yuan-Ting, W. Hui-Long, C. Yao-Rung, Q. Hui-Ping, J. Wen-Feng, Synthesis of baicalin derivatives as eco-friendly green corrosion inhibitors for aluminum in hydrochloric acid solution, *J. Env. Chem. Eng.* 5 (2017) 5891–5901, <https://doi.org/10.1016/j.jece.2017.11.004>.
- [12] M. Abdallah, I.A. Zaafarany, A. Fawzy, M.A. Radwan, E. Abdfattah, Inhibition of aluminum corrosion in hydrochloric acid by cellulose and chitosan, *J. Am. Sci.* 9 (2013) 580–589, <http://www.jofamericanscience.org>.
- [13] G. Babaladimath, V. Badalamoole, S.T. Nandibewoor, Electrical conducting Xanthan Gum-graft-polyaniline as corrosion inhibitor for aluminum in hydrochloric acid, *J. Mater. Chem. Phys.* 205 (2018) 171–179, <https://doi.org/10.1016/j.matchemphys.2017.11.008>.
- [14] K. Khanari, M. Finsgar, M.K. Hrnčić, U. Maver, Z. Knez, Green corrosion inhibitors for aluminum and its alloys, *RSC Adv.* 7 (2017) 2729–2741, <https://doi.org/10.1039/C7RA03944A>.
- [15] N.U. Inbaraj, G.V. Prabhu, Corrosion inhibition properties of paracetamol based benzoxazine on HCS and Al surfaces in 1M HCl, *Prog. Org. Coatings* 115 (2018) 27–40, <https://doi.org/10.1016/j.porgcoat.2017.11.007>.
- [16] O.S.I. Fayomi, I.G. Akande, Corrosion mitigation of aluminium in 3.65%NaCl medium using hexamine, *J. Bio.-Tribo.-Corros.* 5 (2019) 46–54, <https://doi.org/10.1007/s40735-018-0214-4>.
- [17] U.J. Naik, P.C. Jha, M.Y. Lone, N.K. Shah, Electrochemical and theoretical investigation of the inhibitory effect of two Schiff bases of benzaldehyde for the corrosion of aluminum in hydrochloric acid, *J. Mol. Str.* 1125 (2016) 63–72, <https://doi.org/10.1016/j.molstruc.2016.06.054>.
- [18] A. Fawzy, I.A. Zaafarany, H.M. Ali, M. Abdallah, New synthesized amino acids-based surfactants as efficient inhibitors for corrosion of mild steel in hydrochloric acid medium: kinetics and thermodynamic approach, *Int. J. Electrochem. Sci.* 13 (2018) 4575–4600, <https://doi.org/10.20964/2018.05.01>.
- [19] M.F. Gandara, Aluminum: the metal of choice, *Mater. Technol.* 47 (3) (2013) 261–265.
- [20] B.A. Al-Jahdaly, O.A. Al-Malyo, Corrosion inhibition of carbon steel in hydrochloric acid solution using non-ionic surfactants derived from phenol compounds, *Int. J. Electrochem. Sci.* 10 (2015) 2740–2754, <http://www.Electrochem.Sci.org>.
- [21] S.J.H.M. Jessima, A. Berisha, S.S. Srikandan, Preparation, characterization, and evaluation of corrosion inhibition efficiency of sodium lauryl sulfate modified chitosan for mild steel in the acid pickling process, *J. Mol. Liq.* 320 (2020), 114382, <https://doi.org/10.1016/j.molliq.2020.114382>.
- [22] M.G. Acharya, A.N. Shetty, Experimental and theoretical studies on an anionic gemini surfactant as corrosion inhibitor for AZ31 magnesium alloy, *J. Bio.-Tribo.-Corros.* 8 (2022) 91–98, <https://doi.org/10.1007/s40735-022-00687-9>.
- [23] L. Feng, S. Zhang, Y. Qiang, S. Xu, B. Tan, The synergistic corrosion inhibition study of different chain lengths ionic liquids as green inhibitors for X70 steel in acidic medium, *Mater. Chem. Phys.* 215 (2018) 229–241, <https://doi.org/10.1016/j.matchemphys.2018.04.054>.
- [24] D. Wang, Y. Li, B. Chen, L. Zhang, Novel surfactants as green corrosion inhibitors for mild steel in 15% HCl: experimental and theoretical studies, *Chem. Eng. J.* 402 (2020), 126219, <https://doi.org/10.1016/j.ces.2020.126219>.
- [25] A. Yousefi, S. Javadian, M. Sharifi, N. Dalir, A. Motaeae, An experimental and theoretical study of biodegradable gemini surfactants and surfactant/carbon nanotubes (CNTs) mixtures as new corrosion inhibitors, *J. Bio.-Tribo.-Corros.* 5 (2019) 82–94, <https://doi.org/10.1007/s40735-019-0274-0>.
- [26] S.M. Sayyah, S.S. Abd El-Rehim, M.M. El Deeb, S.M. Mohamed, The corrosion inhibition of aluminium by some of 3-alkyloxylaniline monomeric surfactants and their analogues polymers in 0.5 M HCl solution, *Dev. Corros. Prot.* (2014), <https://doi.org/10.5772/57350>.
- [27] I.A. Zaafarany, Nonionic surfactants derived from phenol compound as inhibitor for corrosion of aluminum in hydrochloric acid solution, *J. Electrochem. Plating Technol.* (2014) 1–16, <https://doi.org/10.12850/ISSN2196-0267.JEPT3453>.
- [28] A.Y. EL-Etre, A.H. Tantawy, D.F. Seyam, Corrosion inhibition of aluminium by novel amido-amine based cationic surfactants in 0.5 HCl solution, *J. Surf. Deterg.* 24 (2021) 1–11, <https://doi.org/10.1002/jsde.12546>.
- [29] F.H. Alabdali, M. Abdallah, R. El-Sayed, Corrosion inhibition of aluminum using nonionic surfactant compound with a six membered heterocyclic ring in 1.0 M HCl solution, *Int. J. Electrochem. Sci.* 14 (2019) 3509–3523, <https://doi.org/10.20964/2019.04.59>.
- [30] N.A.F. Al Rawashden, A.K. Maayta, Cationic surfactants as corrosion inhibition for aluminium in acidic and basic solution, *J. Anti-Corrosive Method Mater.* 52 (2005) 160–166, <https://doi.org/10.1108/000355905>.
- [31] N.A. Negem, A.F.M. El-Farargy, E.A. Abdel Halim, S. El-Iboudy, A.El-S.I. Ahmed, Novel bio based nonionic surfactant synthesis, surface activity and corrosion inhibition efficiency against aluminum alloy dissolution in acidic media, *J. Surf. Deterg.* 17 (2014) 1203–1211, <https://doi.org/10.1007/s11743-014-1599-9>.
- [32] R. Mehaoui, A. Khelifa, O. Aaboubi, Inhibition effect of some synthesized surfactants from petroleum oils on the corrosion of aluminum in hydrochloric acid solution, *Res. Chem. Intermed.* 41 (2015) 705–720, <https://doi.org/10.1007/s11164-013-1222-0>.
- [33] M.M. El-Deeb, S.M. Mohamed, Corrosion inhibition of aluminum with a 3-(10-sodium sulfonate decyloxy) aniline monomeric surfactant and its analog polymer in a 0.5M hydrochloric acid solution, *J. Appl. Polym. Sci.* 122 (2011) 3030–3037, <https://doi.org/10.1002/app.34115>.
- [34] M. El Hefnawy, M. Deef Allah, S. Abd El hamed, New biodegradable nonionic-anionic surfactants based on different fatty alcohols as corrosion inhibitors for aluminum in acidic medium, *J. Surf. Deterg.* 24 (2021) 365–379, <https://doi.org/10.1002/jsde.12473>.
- [35] S. Abele, C. Graillat, A. Zicmanis, A. Guyot, Hemiesters and hemiamides of maleic and succinic acid: synthesis and application of surfactants in emulsion polymerization with styrene and butyl acrylate, *Polym. Adv. Technol.* 10 (1999) 301–310. Copyright, 1999 John Wiley & Sons, Ltd.
- [36] F.H. Abd El-Salam, Synthesis, antimicrobial activity and micellization of gemini anionic surfactants in a pure state as well as mixed with a conventional nonionic surfactant, *J. Surf. Deterg.* 12 (2009) 363–370, <https://doi.org/10.1007/s11743-009-1159-x>.
- [37] W. Chen, H.Q. Luo, N.B. Li, Inhibition effect of 2,5-dimercapto-1,3,4-thiadiazole on the corrosion of mild steel in sulphuric acid solution, *Corros. Sci.* 53 (2011) 3356–3365, <https://doi.org/10.1016/j.corsci.2011.06.013>.
- [38] S. Chavda, P. Bahadur, V.K. Aswal, Interaction between nonionic and gemini (cationic) surfactants: effect of spacer chain length, *J. Surf. Deterg.* 14 (2011) 353–362, <https://doi.org/10.1007/s11743-011-1263-6>.
- [39] S.M. Tawfik, Synthesis, surface, biological activity and mixed micellar phase properties of some biodegradable gemini cationic surfactants containing oxycarbonyl groups in the lipophilic part, *J. Ind. Eng. Chem.* 28 (2015) 171–183, <https://doi.org/10.1016/j.jiec.2015.02.011>.
- [40] P.N. Rajarajan, P. Jegannathan, K. Rajeswari, N. Sumathy, A.U. Devi, GC-MS, FTIR and ¹H, ¹³C NMR structural analysis and identification of secondary metabolites from seawater bacterial population, *Asian J. Pharm. Pharmacol.* 5 (2019) 1038–1043, <https://doi.org/10.31024/ajpp.2019.5.6.9>.
- [41] A.M. Elsharif, S.A. Abushait, I. Abdulazeez, H.A. Abubshait, Synthesis, characterization and corrosion inhibition studies of polyunsaturated fatty acid derivatives on the acidic corrosion of mild steel: experimental and computational studies, *J. Mol. Liq.* 319 (2020), 114162, <https://doi.org/10.1016/j.molliq.2020.114162>.
- [42] M.A. Malik, M.A. Hashim, F. Nabi, S.A. Al-Thabaiti, Anti –Corrosion ability of surfactants: A review, *Int. J. Electrochem. Sci.* 6 (2011) 1927–1948.
- [43] S.L. Granese, B.M. Rosales, C. Ovied, J.O. Zerbino, The inhibition action of heterocyclic nitrogen organic compound on Fe and steel, *Corros. Sci.* 33 (1992) 1439–1453, [https://doi.org/10.1016/0010-938X\(92\)90182-3](https://doi.org/10.1016/0010-938X(92)90182-3).
- [44] D. Asefi, M. Arami, A.A. Sarabi, N.M. Mahmoodi, The chain length influence of cationic surfactant and role of nonionic surfactants in controlling the corrosion rate of steel in acidic medium, *Corros. Sci.* 51 (2009) 1817–1821, <https://doi.org/10.1016/j.corsci.2009.05.007>.

- [45] S.A. Umoren, A.A. AlAhmary, Z.M. Gasem, M.M. Solomon, Evaluation of chitosan and carboxymethyl cellulose as ecofriendly corrosion inhibitors for steel, *Int. J. Biol. Macromol.* 117 (2018) 1017–1028, <https://doi.org/10.1016/j.ijbiomac.2018.06.014>.
- [46] D. Chebabe, Z. Ait Chikh, A. Dermaj, K. Rhattas, T. Jazouli, N. Hajjaji, F. El Mdari, A. Srhiri, Synthesis of bolaamphiphile surfactants and their inhibitive effect on carbon steel corrosion in hydrochloric acid medium, *Corros. Sci.* 46 (11) (2004) 2701–2713, <https://doi.org/10.1016/j.corsci.2004.03.016>.
- [47] A. Singh, K.R. Ansari, M.A. Quraishi, H. Lgaz, Y. Lin, Synthesis and investigation of pyran derivatives as acidizing corrosion inhibitors for N80 steel in hydrochloric acid: theoretical and experimental approaches, *J. Alloys Compd.* 762 (2018) 347–362, <https://doi.org/10.1016/j.jallcom.2018.05.236>.
- [48] A.S. Fouda, M.A. Elmorsi, S.M. Shaban, T. Fayed, O. Azazy, Evaluation of N-(3-(dimethyl hexadecyl ammonio)propyl) palmitamide bromide as cationic surfactant corrosion inhibitor for API N80 steel in acidic environment, *Egypt. J. Petrol.* 27 (4) (2018) 683–694, <https://doi.org/10.1016/j.ejpe.2017.10.004>.
- [49] H.M. Abd El-Lateef, K.A. Soliman, A.H. Tantawy, Novel synthesized Schiff Base based cationic gemini surfactants: electrochemical investigation, theoretical modeling and applicability as biodegradable inhibitors for mild steel against acidic corrosion, *J. Mol. Liq.* 232 (2017) 478–498, <https://doi.org/10.1016/j.molliq.2017.02.105>.
- [50] A. Yousefi, S. Javadian, M. Sharifi, N. Dalir, A. Motae, An experimental and theoretical study of biodegradable gemini surfactants and surfactant/carbon nanotubes (CNTs) mixtures as new corrosion inhibitors, *J. Bio.-Tribo.-Corros.* 5 (2019) 82, <https://doi.org/10.1007/s40735-019-0274>.
- [51] M. Yadav, D. Behera, U. Sharma, Nontoxic corrosion inhibitors for N80 steel in hydrochloric acid, *Arab. J. Chem.* 9 (2016) 1487–1495, <https://doi.org/10.1016/j.arabj.2012.03.011>.
- [52] F. Bentiss, M. Lebrini, M. Lagrenée, Thermodynamic characterization of metal dissolution and inhibitor adsorption processes in mild steel/2,5-bis(n-thienyl)-1,3,4-thiadiazoles/hydrochloric acid system, *Corros. Sci.* 47 (2005) 2915–2931, <https://doi.org/10.1016/j.corsci.2005.05.034>.
- [53] Q. Ma, S. Qi, X. He, Y. Tang, G. Lu, 1, 2, 3-Triazole derivatives as corrosion inhibitors for mild steel in acidic medium: experimental and computational chemistry studies, *Corros. Sci.* 129 (2017) 91–101, <https://doi.org/10.1016/j.corsci.2017.09.025>.
- [54] J. Hu, D. Zeng, Z. Zhang, T. Shi, G. Song, X. Guo, 2-Hydroxy-4-methoxy-acetophenone as an environment-friendly corrosion inhibitor for AZ91D magnesium alloy, *Corros. Sci.* 74 (2013) 35–43, <https://doi.org/10.1016/j.corsci.2013.04.005>.
- [55] J. Hu, D. Huang, G. Zhang, G. Song, X. Guo, Research on the inhibition mechanism of tetraphenylporphyrin on AZ91D magnesium alloy, *Corros. Sci.* 63 (2012) 367–378, <https://doi.org/10.1016/j.corsci.2012.06.021>.
- [56] J. Bessone, C. Mayer, K. Juttner, W.J. Lorenz, AC-impedance measurements on aluminium barrier type oxide film, *Electrochim. Acta.* 28 (1983) 171–175, [https://doi.org/10.1016/0013-4686\(83\)85105-6](https://doi.org/10.1016/0013-4686(83)85105-6).
- [57] R.W. Bosch, J. Hubrecht, W.F. Bogaerts, B.C. Syrett, Electrochemical frequency modulation: a new electrochemical technique for online corrosion monitoring, *Corros. Sci.* (2001) 57–60, <https://doi.org/10.5006/1.3290331>.
- [58] D. Chebabe, Z. Ait Chikh, A. Dermaj, K. Rhattas, T. Jazouli, N. Hajjaji, F. El Mdari, A. Srhiri, Synthesis of bolaamphiphile surfactants and their inhibitive effect on carbon steel corrosion in hydrochloric acid medium, *Corros. Sci.* 46 (11) (2004) 2701, <https://doi.org/10.1016/j.corsci.2004.03.016>.
- [59] V.S. Sastri, *Green Corrosion Inhibitors: Theory and Practice*, Wiley, Hoboken, N.J., 2011, p. 310 (Wiley series in corrosion).
- [60] P. Tyagi, R. Tyagi, Synthesis of bisphospho diester surfactants derived from tetradecanol and different methylene chains as a spacer derived from a, x-alkyl dibromides, *J. Tenside Surf. Deterg.* 48 (2011) 293–300, <https://doi.org/10.3139/113.110133>.
- [61] M.J. Rosen, Purification of surfactants for studies of their fundamental surface properties, *J. Colloid Interface Sci.* 79 (1981) 587–598.
- [62] J.S. Leal, J.J. Gonzalez, K.L. Kaiser, V.S. Palabrica, F. Comelles, M.T. Garcia, on the toxicity and biodegradation of cationic surfactant, *Acta Hydrochim. ET Hydrobiol.* 22 (1994) 13–21, <https://doi.org/10.1002/ahch.19940220105>.
- [63] M.M. Motawe, A. El Hossiany, A.S. Fouda, Corrosion control of copper in nitric acid solution using chenopodium extract, *Inter. J. Electrochem. Sci.* 14 (2019) 1372–1381.